Kinetic modelling of network formation and properties in free-radical crosslinking copolymerization

Oguz Okay
TUBITAK Marmara Research Centre, Department of Chemistry, PO Box 21, Gebze, Kocaeli, Turkey
(Received 17 February 1993; revised 2 June 1993)

A kinetic model is presented for the post-gelation period of free-radical monovinyl–divinyl monomer copolymerization reactions. The model involves the moment equations of both the primary and the branched molecules in the sol, and predicts the vinyl-group conversions, the number of crosslinks and the chain-length averages as a function of the reaction time. Formulae for the weight fraction and cycle-rank density of the gel and its equilibrium degree of swelling are derived. The predictions are found to be in good agreement with experimental data on the copolymerization of styrene (S) with *m*-divinylbenzene (DVB) obtained by Hild and Okasha. The reaction time for incipient phase separation during S–DVB copolymerization in the presence of a solvent and the threshold concentration of the DVB for the formation of heterogeneous structures are also calculated.

(Keywords: kinetic modelling; post-gelation period; free-radical copolymerization)

INTRODUCTION

Polymer gels with the ability to absorb many times their dry weight of solvent are widely used as absorbents in medical, chemical and agricultural applications. The properties of the polymer gels, such as their equilibrium swelling ratio and macroporosity, are known to depend on their network structure, and the latter is closely related to their formation history.

Several models have been proposed to describe the formation–structure–properties relationships in polymer gels. The statistical models originate from Flory[1,2] and Stockmayer[3,4], and they all assume equal and conversion-independent reactivities of functional groups[5–8]. However, the free-radical monovinyl–divinyl monomer (MVM–DVM) copolymerization (a commonly used procedure for preparing polymer gels) involves at least three types of functional groups (vinyl groups) with different reactivities, and various elementary reactions[9]. The statistical models are thus not appropriate to deal with such kinetically controlled polymerization systems. An alternative method is to combine kinetic and statistical concepts in modelling MVM–DVM copolymerization[10]: here, the size of the monomer units is increased kinetically to include all of the non-random aspects of the polymerization. Then, the generated 'superspecies' are combined statistically[11–14].

Compared to the statistical models, kinetic models take into account all the kinetic features of copolymerization, and so may offer a more realistic approach to the microscopic phenomena occurring during the MVM–DVM copolymerizations. Kinetic models of MVM–DVM copolymerization involving the moment equations have been proposed by Mikos *et al.*[15], and by Tobita and Hamielec[16–18]. The former model considers the polymer species present in the reaction system as the 'primary molecules'[2], i.e. as the molecules that would result if all crosslinks in the system were cut, and evaluates the moment equations of these hypothetical chains. Although the equations derived are exact as long as the assumptions made are valid, the model cannot predict the properties of sol and gel fractions. Moreover, as also pointed out by Tobita and Hamielec[17], the adaptation of the gel-point condition of the statistical theories into the model is clearly incorrect.

The latter model, the pseudo-kinetic rate-constant method of Tobita and Hamielec, is an excellent model for calculating the chain-length averages of non-linear polymers up to the gel point. However, the moment equations derived for the post-gelation period are quite complex and contain so many kinetic rate constants that a comparison of the model predictions with experiments would be impossible.

The aim of this work was primarily to develop a kinetic model for prediction of sol and gel properties in MVM–DVM copolymerization, such as the chain-length averages of sol molecules, the cycle rank and the equilibrium degree of swelling of the gel, as well as phase separation during crosslinking leading to the formation of porous structures. It was also of inherent interest to derive simple relations between the synthesis conditions and properties of sol and gel fractions for practical calculations.

As is well known, at the gel point many moments of the polymer distribution diverge, so that the passage beyond the gel point is one of the main problems of chemical kinetics. Beyond this point, one may expect that the radicals generated in the sol phase, although reduced in mobility, would still be active, and that they propagate and terminate until becoming a part of the gel. However, radicals located on the gel are enveloped by

0032-3861/94/04/0796–12
© 1994 Butterworth-Heinemann Ltd.

network chains. Although they can react with small molecules, such as primary radicals and monomers, their participation in crosslinking and termination reactions with polymer chains is greatly hindered[19,20]. In the kinetic model presented below, the introduction of the steady-state approximation for sol radicals simplifies the kinetic scheme of the post-gelation period. The equations corresponding to this scheme can be solved analytically to obtain important features of the post-gelation period, such as the weight fraction of gel and the chain-length averages of both primary and branched molecules in the sol. From these features, useful properties of the gel, such as its cycle-rank density and equilibrium degree of swelling, can be readily evaluated.

In the kinetic treatment that follows, the main assumptions made are as follows: (i) the steady-state approximation is assumed for each of the radical species in the sol; (ii) no cyclization reactions occur; (iii) the reactions are chemically controlled before the gel point, and only termination reactions become diffusion-controlled beyond gelation; and (iv) the radicals located on gel molecules are inactive and cannot attack the pendent vinyls. Moreover, in the interests of simplicity: (v) penultimate effects are neglected; (vi) the DVM is assumed to have symmetric vinyls; and (vii) chain transfer reactions are dismissed from the kinetic scheme. However, these latter three points can also be treated with this model.

KINETIC MECHANISM

Vinyl-group conversions

MVM–DVM copolymerization reactions involve three types of vinyl groups, as schematically illustrated in *Figure 1*: (i) those on MVM (M_1), (ii) those on DVM (M_2), and (iii) those on polymer chains, i.e. pendent vinyls (M_3). The instantaneous rate constants for propagation and termination reactions defined as:

$$k_{pi}=\sum_{j=1}^{3} k_{pji}x_j \tag{1a}$$

$$k_{tc}=\sum_{i=1}^{3}\sum_{j=1}^{i} k_{tcij}x_i x_j \tag{1b}$$

$$k_{td}=\sum_{i=1}^{3}\sum_{j=1}^{i} k_{tdij}x_i x_j \tag{1c}$$

$$k_t=k_{tc}+k_{td} \tag{1d}$$

are also shown in *Figure 1*. Here, k_{pji} is the propagation rate constant between radicals and vinyls M_j^* and M_i respectively, k_{tcij} and k_{tdij} are the termination rate constants between radicals of types M_i^* and M_j^* by coupling and by disproportionation respectively, and x_j is the instantaneous mole fraction of the radical M_j^*, i.e. $x_j=[M_j^*]/[R^{\bullet *}]$, where $[R^{\bullet *}]$ is the total radical (active primary molecule) concentration defined by:

$$[R^{\bullet *}]=\sum_{j=1}^{3}[M_j^*]$$

Note that the instantaneous rate constants defined above are equivalent to the pseudo-kinetic rate constants in the formalism of Tobita and Hamielec[18]. The instantaneous mole fraction of the radical species x_j can easily be evaluated as in a terpolymerization[21] (see Appendix 1). Applying equations (1a)–(1d), one may derive the rate equations for the concentration of the initiator I, vinyl groups M_i and crosslinks μ as follows:

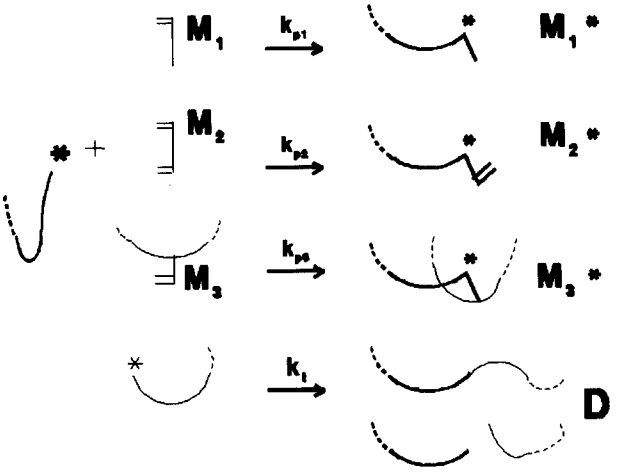

Figure 1 Scheme of propagation and termination reactions in free-radical copolymerization of a MVM with a DVM having symmetric vinyls

$$r_I=-k_d[I] \tag{2}$$

$$r_{M_1}=-k_{p1}[R^{\bullet *}][M_1] \tag{3}$$

$$r_{M_2}=-2k_{p2}[R^{\bullet *}][M_2] \tag{4}$$

$$r_{M_3}=k_{p2}[R^{\bullet *}][M_2]-k_{p3}[R^{\bullet *}][M_3] \tag{5}$$

$$r_\mu=k_{p3}[R^{\bullet *}][M_3] \tag{6}$$

$$[R^{\bullet *}]=(2fk_d[I]/k_t)^{1/2} \tag{7}$$

where k_d is the decomposition rate constant of the initiator and f is the initiator efficiency.

Since, according to the proposed model, the reactions occurring before the gel point are assumed to be chemically controlled, all the rate constants of the elementary reactions are constant quantities up to the gel point. However, beyond gelation, termination reactions become strongly diffusion-controlled owing to the decrease in the mobility of the polymer radicals and to the steric hindrance of the network chains. As a result, the rate constant k_t will decrease continuously as the polymerization proceeds, and one may expect that this decrease depends on the crosslink density of the reaction system[19]. The apparent decrease of the termination rate of the radicals beyond gelation may be given by the empirical relation:

$$k_t=z(\varepsilon)k_t^0 \tag{8}$$

where k_t^0 represents the chemically controlled termination rate constant and $z(\varepsilon)$ is a function describing the variation of the termination rate with the crosslink density. There is presently no theory available to give the functional form of $z(\varepsilon)$. Therefore, it can be estimated by fitting experimental data of the post-gelation period.

Molecular-weight distribution of sol molecules

Depending on the location, the proposed kinetic model distinguishes two types of radicals, polymers and vinyl groups: those in the sol and those on the gel. Henceforth, symbols with a prime (′) or double prime (″) are used to denote species in the sol or in the gel, respectively, whereas those without any primes refer to species in the whole polymerization system. Neglecting the attack of gel radicals on pendent vinyl groups, the equations for the appearance and disappearance of sol molecules

composed of r structural units can be written as follows:

Formation

$$A^* + M'_{i,r-1} \xrightarrow{k_{ai}} R'^*_r \quad (9a)$$

$$R'^*_{r-j-1} + M'_{i,j} \xrightarrow{k_{pi}} R'^*_r \quad (r > j+1) \quad (9b)$$

$$R'^*_s + R'^*_{r-s} \xrightarrow{k_{tc}} D'_r \quad (r > s) \quad (9c)$$

Consumption

$$R'^*_r + M_{i,j} \xrightarrow{k_{pi}} R^*_{r+j+1} \quad (9d)$$

$$M'_{i,r} + R'^*_s \xrightarrow{k_{pi}} R'^*_{r+s+1} \quad (9e)$$

$$R'^*_r + R^*_s \xrightarrow{k_t} D_{r+s} \text{ and/or } D_r + D_s \quad (9f)$$

($r, s = 1, 2, 3, \ldots$; $j = 0, 1, 2, \ldots$; $i = 1, 2$ and 3)

Here A^* is the primary radical, k_{ai} is the initiation rate constant with vinyl M_i, $M_{i,j}$ represents the vinyl group of type i belonging to a molecule composed of j structural units, and R^*_r and D_r represent the active polymer and the dead polymer of chain length r, respectively. Since, in the pre-gelation period, only finite species are present in the reaction system, the concentration of sol species is equal to their overall concentration, i.e. $[R'^*_r] = [R^*_r]$. Beyond the gel point, a large number of sol molecules are still present in the reaction system. They become connected to the infinite network (gel) as the crosslinking reactions proceed. Experimental data clearly show that the decrease in the crosslink density of the sol just beyond the gel point is very rapid. Over a wide conversion range, the average chain length of the sol species remains almost constant[2,9,22–24]. Accordingly, one may expect that the concentration of sol radicals should decrease very rapidly at the gel point, but the rate of change of the sol radical concentration should quickly become and remain zero during the course of the post-gelation period (steady-state condition for sol radicals).

Relying on the above hypothesis, the method of moments can be applied to the kinetic model of the reactions represented by equations (9a)–(9f) to calculate the nth moment of the active polymer and the polymer distributions in the sol, defined as:

$$Y_n \equiv \sum_{r=1}^{\infty} r^n [R'^*_r] \quad (10a)$$

$$Q_n \equiv \sum_{r=1}^{\infty} r^n [P'_r] \quad (10b)$$

respectively. Here, P'_r denotes the (active + dead) sol polymers of chain length r, i.e. $[P'_r] = [R'^*_r] + [D'_r]$. From the moments of the distribution, the nth average chain length of the active polymer and that of the total polymer in the sol can be calculated as follows:

$$\bar{X}^*_n = Y_n / Y_{n-1} \quad (11a)$$

$$\bar{X}_n = Q_n / Q_{n-1} \quad (11b)$$

In the following treatment, symbols with a superscript dot (*) relate to the primary molecules, whereas those without this superscript relate to the branched molecules.

Moments of the primary molecules

If the primary molecules are considered as the sole reacting species, the kinetic treatment of MVM–DVM copolymerization is extremely simplified because $j = 0$ for all vinyl groups $M'_{i,j}$. The preceding reaction scheme can be adapted to this treatment merely by replacing $M'_{i,j}$ with $M'_{i,0}$ and eliminating equation (9e). From the balance equations given in Appendix 2, the moments of the primary molecules can be expressed as follows:

$$Y^*_n = n!(Y^*_1/Y^*_0)^n Y^*_0 \qquad n = 2, 3, 4, \ldots \quad (12)$$

$$r_{Q^*_n} = \left(\frac{k_{td}}{\phi_s} + \frac{n+1}{2} k_{tc}\right) Y^*_0 Y^*_n \qquad n = 0, 1, 2, \ldots \quad (13)$$

where

$$Y^*_0 = \phi_s [R^{\bullet *}]$$

$$Y^*_1 = \phi_s^2 \sum_{i=1}^{3} k_{pi} [M_i] / k_t$$

and ϕ_s is the fraction of radicals belonging to the sol fraction:

$$\phi_s = \left(1 + \frac{k_{p3}[M''_3]}{k_t [R^{\bullet *}]}\right)^{-1} \quad (14)$$

The moment equations allow calculation of the chain-length averages of the primary molecules in the sol, i.e. the nth average chain length of polymer radicals in the sol:

$$\bar{X}^{\bullet *}_n = n Y^*_1 / Y^*_0 \qquad n = 1, 2, 3, \ldots \quad (15)$$

and the instantaneous nth average chain length of the primary molecules in the sol ($X^*_n = r_{Q^*_n} / r_{Q^*_{n-1}}$):

$$X^*_n = \left(\frac{k_{td}/\phi_s + \frac{1}{2}(n+1)k_{tc}}{k_{td}/\phi_s + \frac{1}{2}n k_{tc}}\right) \bar{X}^{\bullet *}_n \qquad n = 1, 2, 3, \ldots \quad (16)$$

On the basis of the distribution moments, some useful properties of network-forming systems may now be defined. The average crosslink density of the sol polymer, $\bar{\rho}'$, which is the fraction of branched structural units in the sol, is:

$$\bar{\rho}' = 2[\mu']/Q^*_1 \quad (17)$$

and the number of branched units per weight-average primary molecule in the sol, $\bar{\varepsilon}'$, is:

$$\bar{\varepsilon}' = \bar{\rho}' \bar{X}^*_2 \quad (18)$$

Note that, by setting $\phi_s = 1$, the equations given above predict the properties of the primary molecules prior to gelation, or their average properties in the whole reaction system (sol + gel) beyond gelation. For example, the overall crosslink densities can be calculated as follows:

$$\bar{\rho} = 2[\mu]/Q^*_{1,\phi_s=1} \quad (17a)$$

$$\bar{\varepsilon} = \bar{\rho} \bar{X}^*_{2,\phi_s=1} \quad (18a)$$

Moments of the branched molecules

In contrast to the primary molecules, the polymerization degree of a branched molecule changes upon reaction of pendent vinyls belonging to it with radicals (equation (9e)). Thus, the chain length j is zero for monomeric vinyls M_1 and M_2 but larger than zero for pendent vinyls M_3. The quantitative treatment of the reactions based on branched molecules also requires two assumptions. First,

the rate at which a radical reacts with a polymer to form a branch point is proportional to the number of units of the polymer; in other words, the distribution of units bearing pendent vinyls along the polymer is homogeneous, i.e.:

$$[M'_{3,r}]=([M'_3]/Q_1)r[P'_r] \tag{19}$$

In fact, this approximation is equivalent to stating that, according to the terminology of the Tobita–Hamielec crosslink-density distribution model[17,18,25,26], the additional crosslink density $\rho_a(\theta, \psi)$ is independent of the birth conversion θ. The second assumption stipulates that only one radical centre is present in each active polymer ($Y_0 = Y_0^\bullet$), i.e. crosslinks are assumed to form only between polymer chains born at different conversions.

From equations (A6) and (A8) of Appendix 2, the moments for branched molecules in the sol can be expressed as follows:

$$Y_n = n\left(\frac{Y_1^\bullet}{Y_0}\right)Y_{n-1} + \frac{k_{p3}[M'_3]}{k_t Y_0 Q_1}\phi_s^2 \sum_{\nu=0}^{n-1}\binom{n}{\nu} Y_\nu Q_{n+1-\nu} \qquad n=1,2,3,\ldots \tag{20}$$

$$r_{Q_0} = r_{Q_0^\bullet} - k_{p3}[M'_3]Y_0 \tag{21a}$$

$$r_{Q_1} = r_{Q_1^\bullet} \tag{21b}$$

$$r_{Q_2} = 2(k_{td}/\phi_s + 1.5k_{tc})Y_1^2 - k_{p3}[M'_3]Y_0(W_g/\phi_s)Q_3/Q_1 \tag{21c}$$

$$r_{Q_n} \simeq n[k_{td}/\phi_s + \tfrac{1}{2}(n+1)k_{tc}]Y_1 Y_{n-1} \qquad n=3,4,5,\ldots \tag{21d}$$

where W_g is the gel fraction.

The nth average polymerization degree of active polymers is given by:

$$\bar{X}_n^* = \bar{X}_n^{\bullet *} + \frac{k_{p3}[M'_3]}{k_t Y_0 Y_{n-1} Q_1}\phi_s^2 \sum_{\nu=0}^{n-1}\binom{n}{\nu} Y_\nu Q_{n+1-\nu} \qquad n=1,2,3,\ldots \tag{22}$$

The instantaneous nth average polymerization degree of the branched molecules is:

$$(X_1)^{-1} = (X_1^\bullet)^{-1} - \rho' \tag{23a}$$

$$X_2 = X_2^\bullet(1+\rho'\bar{X}_2)^2 \simeq X_2^\bullet(1+2\rho'\bar{X}_2) \qquad \text{for } \rho' \ll 1 \tag{23b}$$

$$X_n \simeq (\bar{X}_{n-1}^*/\bar{X}_{n-1}^{\bullet *})X_n^\bullet \qquad n=3,4,5,\ldots \tag{23c}$$

where ρ' is the instantaneous crosslink density of sol molecules, i.e. $\rho' = \mathrm{d}[\mu']/\mathrm{d}Q_1$. The first and second average polymerization degrees of the accumulated sol polymer can be obtained from equations (23a) and (23b) as:

$$(\bar{X}_1)^{-1} = (\bar{X}_1^\bullet)^{-1} - 0.5\bar{\rho}' \tag{23a'}$$

$$\bar{X}_2 = \frac{\bar{X}_2^\bullet}{1-(2/Q_1)\int_0^{Q_1}\rho' X_2^\bullet \,\mathrm{d}Q_1} = \frac{\bar{X}_2^\bullet}{1-\bar{\varepsilon}'} \tag{23b'}$$

which are identical to the equations derived by Flory and Stockmayer using statistical methods[2,4]. (Note that the symbols marked by a superscript bar denote the accumulated values, i.e. $\bar{\rho}' = (2/Q_1)\int_0^{Q_1}\rho' \,\mathrm{d}Q_1$.) Moreover, by setting $\phi_s = 1$ and $W_g = 0$, all the above equations describe the properties of the branched molecules prior to gelation, and they are identical to the equations of the Tobita–Hamielec model[17].

Gelation

The presence of pendent vinyl groups on the growing polymer species offers the possibility of forming chemical structures of macroscopic dimensions called polymer gels. At the incipient formation of infinite structures, which is defined as the gel point, the second average polymerization degree goes to infinity:

$$(\bar{X}_2)^{-1} = 0 \tag{24}$$

Moreover, the gel point can also be predicted after substitution of equation (24) into equation (23b') as:

$$\bar{\varepsilon}' = 1 \tag{25a}$$

so that the average crosslink density at the gel point becomes:

$$\bar{\rho}' = 1/\bar{X}_2^\bullet \tag{25b}$$

which is identical with the Flory–Stockmayer criterion for the onset of gelation. It must be pointed out that the dependence of the crosslink-density distribution on the birth conversion of the primary chains is not accounted for in the present model. Actually, gelation occurs earlier, i.e. $\bar{\varepsilon}'$ is less than unity at the gel point, if there is a crosslink-density distribution among the primary chains[9]. In order to remove this approximation, ρ' in equation (23b') should be replaced with ρ'_w, which is the instantaneous weight-average crosslink density of the primary chains[9].

Weight fraction of sol (W_s)

The weight fraction of soluble polymer in the reaction mixture is defined by

$$W_s \equiv Q_1^\bullet / Q_{1,\phi_s=1}^\bullet \tag{26}$$

and can be calculated from equation (13) as:

$$W_s = \phi_s^2[1-(k_{tc}/k_t)(1-\phi_s)] \tag{27}$$

In order to solve equation (27) together with equation (14), one needs to know the concentration of pendent vinyls in the gel ($[M''_3]$). The statistical theory of network formation predicts the ratio of the crosslink densities in the gel and in the entire system as[2]:

$$\bar{\rho}''/\bar{\rho} \simeq 1 + W_s \tag{28a}$$

whereas the kinetic model gives, assuming random crosslinking:

$$\frac{\bar{\rho}''}{\bar{\rho}} = \frac{[\mu'']}{[\mu]W_g} = \frac{[M''_3]}{[M_3]W_g} \tag{28b}$$

From these equations one obtains:

$$[M''_3] = [M_3](1-W_s^2) \tag{29}$$

and substituting this relation and equation (14) into equation (27) yields:

$$\frac{1-W_s^a}{W_s^a(1-W_s^2)} = 0.5a\bar{\varepsilon} \tag{30}$$

where $a=(2+k_{tc}/k_t)^{-1}$. Equation (30) predicts the gel fraction from the overall crosslink density of the reaction system.

GEL PROPERTIES

Cycle rank

A polymer network can be best characterized by its cycle rank, ξ, defined as the number of independent circuits in it, or as the number of chains that have to be cut to reduce the network to a macroscopic tree[27]. Assuming random crosslinking, the macroscopic tree-like structure first formed in MVM–DVM copolymerization contains no closed circuit. Thus, at the time of gelation, the cycle rank of the network is zero. After gelation, closed circuits start to form in the network structure, and each active crosslink will produce, on average, one independent circuit. Accordingly, the instantaneous network structures formed in MVM–DVM copolymerization can be considered as occurring in two steps.

In the first step, all the primary molecules of the network are joined to form a macroscopic tree with $\xi=0$. The number density of active crosslinks at the end of the first step, $[\mu_1'']/Q_1''^{\bullet}$, can be calculated using equations (25b) and (28a) as:

$$[\mu_1'']/Q_1''^{\bullet}=(\bar{X}^{\bullet}_{2,\phi_s=1})^{-1} \tag{31}$$

where $Q_1''^{\bullet}$ is the first moment of the primary molecule distribution of the gel.

In the second step, additional crosslinks are introduced intermolecularly. Since the total number density of active crosslinks in the final network is known from equation (28) and can be written as:

$$[\mu'']/Q_1''^{\bullet}=[\mu](1+W_s)/Q^{\bullet}_{1,\phi_s=1} \tag{32}$$

the number density of additional crosslinks produced in the second step, $([\mu'']-[\mu_1''])/Q_1''^{\bullet}$, is equal to the cycle-rank density of the network:

$$\frac{\xi}{Q_1''^{\bullet}}=\frac{[\mu](1+W_s)}{Q^{\bullet}_{1,\phi_s=1}}-\frac{1}{\bar{X}^{\bullet}_{2,\phi_s=1}} \tag{33}$$

Equilibrium degree of swelling

Flory's swelling equation for tetrafunctional networks[28]:

$$\ln(1-v_2)+v_2+\chi v_2^2=-(\xi/V_0)\bar{V}_1 v_2^{1/3}(v_2^{\circ})^{2/3}(1+K) \tag{34}$$

is used for interpreting the swelling behaviour of the networks obtained in MVM–DVM copolymerization. Here, v_2 is the volume fraction of the network in the equilibrium swollen gel, χ is the polymer–solvent interaction parameter, V_0 is the volume of the network in the reference state, $\bar{V}_1$ is the molar volume of solvent, v_2° is the volume fraction of the gel at the end of its formation (i.e. $v_2^{\circ}=Q_1''^{\bullet}\bar{V}_2$), $\bar{V}_2$ is the molar volume of the structural unit, and K is a factor. K is a function of v_2 and also of the network parameter κ, which is a measure of entanglement constraints. The two extreme cases for K are 0 and $1-v_2^{2/3}$ respectively for phantom and affine networks[29].

The polymer–solvent interaction parameter χ in general depends on v_2 and on the temperature. At constant temperature, this dependence is given by[30]:

$$\chi=\chi_1+\chi_2 v_2+\chi_3 v_2^2+\cdots \tag{35}$$

where χ_1, χ_2, χ_3, ... are empirical constants.

In the notation of the thermodynamic theories of polymer solutions and thus in the derivation of the left-hand side of equation (34), a polymer chain is considered as a collection of hypothetical repeat units called segments; a segment is defined as the portion of a chain whose volume equals that of the solvent molecule[2]. For coupling equation (34) to the model, a structural unit and a segment are assumed to be identical. Thus, since $V_0=Q_1''^{\bullet}\bar{V}_1$, the cycle-rank density of the network with respect to the network volume is obtained from equation (33) as:

$$\frac{\xi}{V_0}=\frac{1}{\bar{V}_1}\left(\frac{[\mu](1+W_s)}{Q^{\bullet}_{1,\phi_s=1}}-\frac{1}{\bar{X}^{\bullet}_{2,\phi_s=1}}\right) \tag{36}$$

Using equations (34)–(36), the equilibrium degree of swelling of the network in the reaction system, i.e. in the mixture of the monomers, solvent and the sol molecules, or in a swelling agent, can be calculated as a function of the post-gelation time.

Phase separation

Both the equilibrium degree of swelling of the gel in the reaction system (v_2^{-1}) and its degree of dilution ($(v_2^{\circ})^{-1}$) decrease as the reaction time increases and, after a definite time, v_2 may reach the value of v_2°. Thereafter, since dilution of a gel cannot be greater than its equilibrium degree of swelling, the excess of the diluent (unreacted monomers plus solvent) should separate out of the gel phase, resulting in the syneresis of the gel, i.e. in phase separation[31]. Thus, the condition for incipient phase separation during MVM–DVM copolymerization is given by:

$$v_2=v_2^{\circ} \tag{37}$$

After phase separation, v_2 increases with further crosslinking but the actual degree of dilution of the gel in the reaction system, i.e. its degree of solvation, should remain equal to v_2. Thus, assuming the validity of the limitations following from the Flory lattice theory and the theory of rubber elasticity, equation (34) becomes after phase separation:

$$\ln(1-v_2)+v_2+\chi v_2^2=-(\xi/V_0)\bar{V}_1 v_2(1+K) \tag{38}$$

Moreover, since $(v_2^{\circ})^{-1}-(v_2)^{-1}$ equals the volume ratio of the diluent to the gel phase (V_d), the porosity of the networks after removing the diluent and after drying, $P\%$, can also be calculated. Assuming isotropic swelling, it is given by:

$$P\%=\frac{V_d}{1+V_d}\times 100 \tag{39}$$

It must be pointed out that the isotropic swelling assumption is equivalent to stating that V_d does not change when a gel molecule is dried. However, as is well known from recent studies, the drying process of a gel molecule may lead to a partial or total collapse of the pores[32,33]. The preservation of the original porosity, called 'maximum porosity', can be attained by decreasing the interactions between polymer chains and the solvent before the drying process, i.e. during the treatment of swollen gel with solvents with decreasing solvating power[33]. Accordingly, $P\%$ predicted by the model corresponds to the maximum porosity of the networks.

End of the copolymerization

MVM–DVM copolymerization reactions can end before total conversion of vinyl groups, when the reaction temperature (T) is below the glass transition temperature of the reaction system (T_{g12}). Experimental data show that the glass transition temperature of a polymer network (T_{g1}) increases as its crosslink density increases[34]. This dependence can be given by the empirical relation:

$$T_{g1} = T_{g10} + AX_2 + B(X_2)^2 + \cdots \quad (40)$$

where T_{g10} is the glass transition temperature of the primary molecule, X_2 is the mole fraction of the DVM in the network, and A, B, ... are constants. For example, analysis of the measurements of Ellis *et al.*[35] leads to the following expression for T_{g1} of styrene–divinylbenzene networks:

$$T_{g1}\ (\mathrm{K}) = 385 + 135X_2 + 183(X_2)^2 \quad (41)$$

On the other hand, the glass transition temperature of a polymer network–solvent system (T_{g12}) can be calculated using the equation[35]*:

$$T_{g12} = \frac{v_2^\circ \Delta C_{p1} T_{g10} + (1 - v_2^\circ)\Delta C_{p2} T_{g2}}{v_2^\circ \Delta C_{p1} T_{g10}/T_{g1} + (1 - v_2^\circ)\Delta C_{p2}} \quad (42)$$

where ΔC_{p1} and ΔC_{p2} are the incremental changes in the heat capacities of the primary molecules and the solvent at their T_g respectively, and T_{g2} is the glass transition temperature of the solvent.

Taking $T_{g12} = T$, equations (40) and (42) can be solved for v_2° to predict the end-point of the MVM–DVM copolymerization reactions.

Calculations

The kinetic model is solved for a batch isothermal MVM–DVM copolymerization. Owing to the differences in the densities of the MVM (d_1), DVM (d_2) and the polymer (d_p), the reaction volume V_r will change during the polymerization. If S represents the concentration of species I, M_i, μ and the moments of the polymer distributions Q_n, a mass balance requires:

$$r_S = \frac{\mathrm{d}(V_r S)}{V_r\,\mathrm{d}t} = \frac{\mathrm{d}S}{\mathrm{d}t} + \frac{S}{V_r}\frac{\mathrm{d}V_r}{\mathrm{d}t} \quad (43)$$

where $\mathrm{d}V_r/\mathrm{d}t$ is the rate of volume change, which, assuming ideal solutions, is given by:

$$\mathrm{d}V_r/\mathrm{d}t = [r_{M_1}(d_1^{-1} - d_p^{-1})MW_1 + 0.5 r_{M_2}(d_2^{-1} - d_p^{-1})MW_2]V_r \quad (44)$$

where MW_1 and MW_2 are the molecular weights of MVM and DVM respectively.

The mass-balance equations of the kinetic model represented by equation (43) can be solved numerically to predict the conversions, number of active crosslinks, average polymerization degrees of the primary molecules as well as of the branched molecules, and the characteristics of the networks such as the cycle-rank density and the equilibrium degree of swelling as a function of the polymerization time. The gel fraction can be calculated using equation (30) from the overall crosslink density of the reaction system, and equations (16) and (23) serve for the evaluation of the average polymerization degrees of sol species beyond the gel point.

* In ref. 35, T_{g12} is expressed in terms of different parameters than given in equation (42). The correspondences are $T_{g1}(X=0) = T_{g10}$, $T_{g1}(X) = T_{g1}$, $\Delta C_{p1}(X=0) = \Delta C_{p1}$, $x_1 = v_2^\circ$, and $x_2 = 1 - v_2^\circ$

RESULTS AND DISCUSSION

The kinetic model was solved for the styrene–*m*-divinylbenzene (S–*m*-DVB) copolymerization in benzene solutions at 60°C using 2,2′-azobisisobutyronitrile (AIBN) as an initiator. The predictions of the model were compared with the experimental data of Hild and Okasha[24,36]. The values of the kinetic constants and the parameters used in the calculations are given in *Table 1*. The propagation, crosslinking and termination rate constants are assumed to be independent of the type of the radical end, i.e. $k_{p11} = k_{p21} = k_{p31}$. The chain transfer reactions are neglected because of the very low transfer constants to the monomers and to the selected solvent[21]. The functional form of $z(\varepsilon)$ describing the decrease in the termination rate constants beyond gelation was estimated from the variation of gel properties with the reaction time. The empirical correlation:

$$z(\varepsilon) = m \Big/ \sum_{i=1}^{m} \varepsilon^i \quad (45)$$

was found to be best suited to fit the experimental data of Hild and Okasha. Here m is an adjustable parameter, which can take on integral values.

The factor K of the swelling equation (equation (34)) is taken to be zero (phantom network assumption). Benzene, toluene, styrene and divinylbenzene have similar thermodynamic properties; moreover the polystyrene/S–DVB network interaction parameter is negligible[40]. Thus, using the values of the empirical constants χ_i given in *Table 1*, which are reported to be temperature-independent, the equilibrium swelling degrees of S–DVB networks in the polymerization system or in the swelling agent toluene or benzene can be calculated by use of equation (34) (for $v_2 < v_2^\circ$) or of equation (38) (for $v_2 > v_2^\circ$).

The rate constant of the intermolecular crosslinking reactions k_{pj3} was calculated using the experimental gelation time measured by Hild and Okasha[36] for the following reaction conditions: $[M_1]_0 = 4$ M; $[M_2]_0 = 0.16$ M; $[I]_0 = 0.08$ M; $c = 43\%$ (initial mass of the monomers in 100 ml solution); DVB = 2% (mol% of

Table 1 Kinetic constants and parameters for S–*m*-DVB copolymerization in benzene at 60°C using AIBN as an initiator

Constants		Ref.
k_d	$= 8.5 \times 10^{-6}\ \mathrm{s}^{-1}$	21
k_{pj1}	$= 145\ \mathrm{l\,mol^{-1}\,s^{-1}}$	21[a]
k_{pj2}	$= 165\ \mathrm{l\,mol^{-1}\,s^{-1}}$	36
k_{tcij}	$= 2.9 \times 10^7\ \mathrm{l\,mol^{-1}\,s^{-1}}$	21[a]
k_{tdij}	$= 0$	21[a]
f	$= 0.45$	36
χ_1	$= 0.455$	37, 38[b]
χ_2	$= -0.155$	37, 38[b]
χ_i	$= 0\ (i \geq 3)$	37, 38[b]
ΔC_{p1}	$= 0.283\ \mathrm{J\,g^{-1}\,K^{-1}}$	35
ΔC_{p2}	$= 0.70\ \mathrm{J\,g^{-1}\,K^{-1}}$	35
T_{g10}	$= 385$ K	35
T_{g2}	$= 113$ K	39
$d_1 = d_2$	$= 0.91\ \mathrm{g\,ml^{-1}}$	
MW_1	$= 104\ \mathrm{g\,mol^{-1}}$	
MW_2	$= 130\ \mathrm{g\,mol^{-1}}$	
d_p	$= 1.08\ \mathrm{g\,ml^{-1}}$	33

[a] Rate constant for the homopolymerization of styrene
[b] Constant for S–DVB network/toluene system

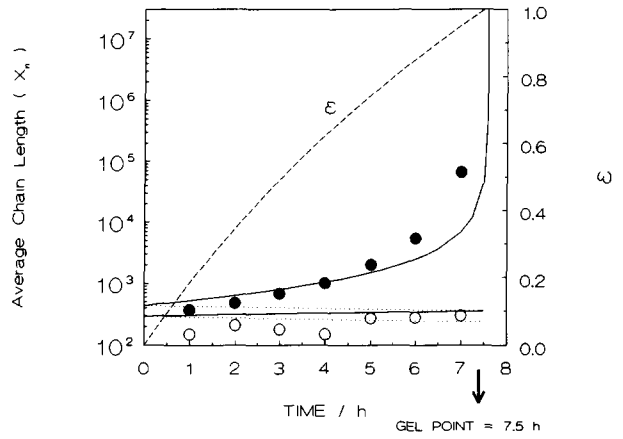

Figure 2 Average polymerization degrees of the primary molecules $\bar{X}_n^*$ (dotted curves), the branched molecules $\bar{X}_n$ (full curves) and the crosslink density in terms of $\bar{\varepsilon}$ (dashed curve) plotted as functions of the reaction time up to the gel point for S–*m*-DVB copolymerization in benzene at 60°C using AIBN as an initiator. $n=1$ and 2 for the lower and upper curves of each series respectively. The filled and empty circles show the results of the measurements of Hild and Okasha for $\bar{X}_2$ and $\bar{X}_1$ respectively. $c=43\%$, DVB = 2% and $[I]_0=0.08$ M

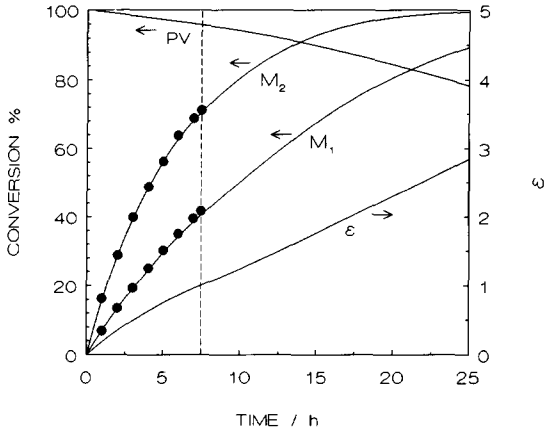

Figure 3 Vinyl-group conversions, fraction of the DVB units bearing pendent vinyl groups *PV*, and $\bar{\varepsilon}$ shown as functions of the reaction time. Experimental results of Hild and Okasha are shown as filled circles. Calculations beyond gelation are for $m=2$. The broken vertical line represents the position of the gel point. See legend to *Figure 2* for the reaction conditions

m-DVB with respect to the monomers). Here the subscript 0 indicates initial concentrations. They found a gelation time of 7.5 h. The kinetic model predicts the onset of gelation after 7.5 h if k_{pj3} is 191 $mol^{-1}\,s^{-1}$. This value was used for further calculations.

For the initial conditions given above, *Figure 2* shows the number- and weight-average polymerization degrees and the $\bar{\varepsilon}$ value as functions of the reaction time up to the gel point. The dotted curves represent the average polymerization degrees of the primary molecules ($\bar{X}_n^*$), whereas the full curves represent those of the branched molecules ($\bar{X}_n$). For the lower and upper curves of each series, $n=1$ and 2, respectively. The filled and empty circles are the results of the measurements of Hild and Okasha for $\bar{X}_2$ and $\bar{X}_1$ respectively. The predictions of the model are in good agreement with the experimental results. Deviations appearing between the theoretical and experimental $\bar{X}_2$ values as time approaches the gelation time may be due to the increase in the number of radical centres per living polymer.

For the same reaction conditions, the vinyl-group conversions, the fraction of DVB units bearing pendent vinyls (*PV*) and $\bar{\varepsilon}$ are plotted against the reaction time in *Figure 3*. The adjustable parameter *m* representing the extent of autoacceleration in the post-gelation period is assumed equal to 2. Experimental conversion data of Hild and Okasha up to the gel point are also shown as filled circles. Again, the predictions of the model are in excellent agreement with the experimental results, although the overall conversion at the gel point is unusually high (about 40%). Therefore, one may conclude that the assumption of the model that the reactions in the pre-gelation period are chemically controlled is correct, at least for the system studied. The consumption rates of the vinyl groups and the formation rate of crosslinks increase beyond gelation owing to the increase in the radical concentration according to equations (7) and (8), i.e. owing to the gel effect.

In *Figure 4a*, the number- and weight-average polymerization degrees prior to gelation and for the sol after gelation are shown as functions of the reaction time. The chain-length averages of the primary molecules (dotted curves) decrease only slightly during the course of the polymerization, whereas the weight-average polymerization degree of the branched molecules is a hyperbolic function of the pre-gelation time. Beyond the gel point, the weight-average polymerization degree of the sol $\bar{X}_2$ returns to finite values and both $\bar{X}_1$ and $\bar{X}_2$

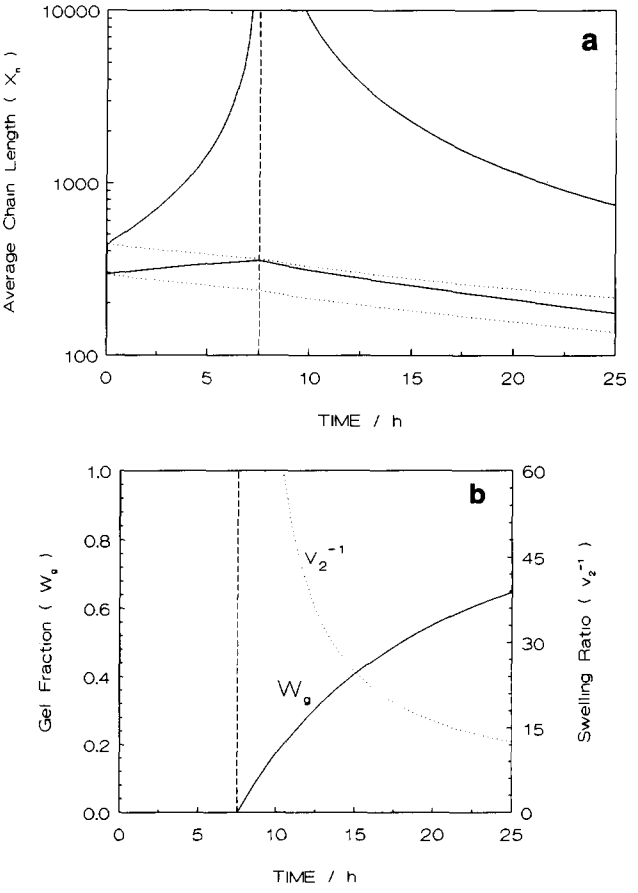

Figure 4 (a) Variation of the average polymerization degrees of the primary molecules (dotted curves) and the branched molecules (full curves) with the reaction time. (b) Variation of the gel fraction W_g and the equilibrium swelling ratio of the gel in toluene v_2^{-1} with the reaction time. Calculations are for $m=2$. See legend to *Figure 2* for the reaction conditions

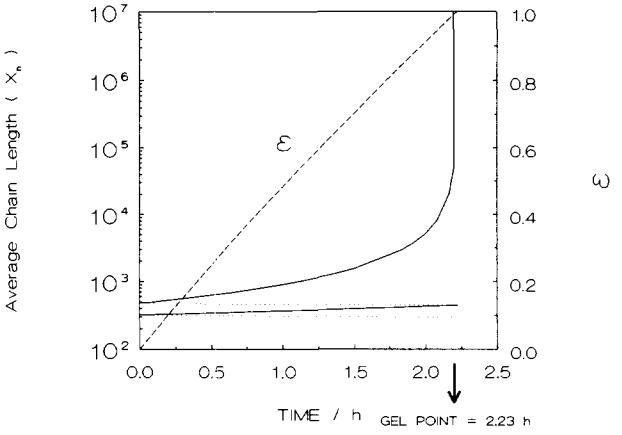

Figure 5 Variation of the average polymerization degrees and $\bar{\varepsilon}$ with the reaction time up to the gel point. DVB = 5%, c = 43%, $[I]_0$ = 0.08 M. See legend to *Figure 2*

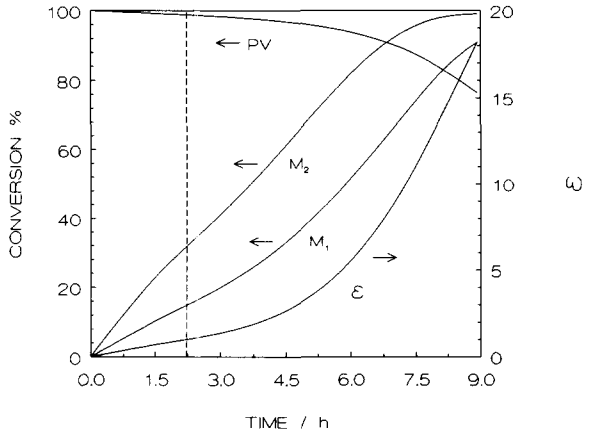

Figure 6 Vinyl-group conversions and $\bar{\varepsilon}$ shown as functions of the reaction time for 5% DVB. c = 43%, $[I]_0$ = 0.08 M. The broken vertical line represents the gel point

decrease with further crosslinking. *Figure 4b* shows the dependence of the gel fraction W_g and the equilibrium volume swelling ratio ($1/v_2$) of the gel in toluene on the reaction time. The rate of change in W_g and in the swelling ratio is rapid beyond gelation up to 15 h; thereafter, it slows down owing to the small amount of crosslinking agent set in and as a result of the low rate constant of the crosslinking reactions.

For 5% DVB, Hild *et al.*[24] reported a gelation time of 3.25 h compared to 2.23 h predicted by the model, as seen in *Figure 5*. The deviation between theory and experiment in the gelation times can be attributed to the intramolecular crosslinking reactions. The variation of the vinyl-group conversions and $\bar{\varepsilon}$ with time are shown in *Figure 6*. Compared to *Figure 3*, the increase in the DVB concentration from 2 to 5% shifts the gel point t_g to lower conversion (from 40 to 16%) and enhances the effect of autoacceleration.

Under the same reaction conditions, the variations of the gel properties and the average polymerization degrees of the species with the reaction time are shown in *Figure 7*. The experimental results of Hild *et al.*[24] are also shown as data points. In spite of the differences between the measured and calculated gelation times, the experimental values agree well with the theoretical curves. Experiments indicate that the cyclization reactions lead to a decrease in the average polymerization degree, a decrease in the gel fraction and an increase in the equilibrium degree of swelling[41,42]. As seen in *Figure 7*, these are also the trends of the slight deviations between theory and experiment. *Figure 7b* also shows that, as the gel fraction approaches unity, the average polymerization degree of the branched molecules becomes equal to that of the primary molecules, indicating that only linear chains and unreacted styrene constitute the sol fraction towards the end of the polymerization.

The effect of the initial DVB concentration on the critical conversion of the vinyl groups at t_g is shown in *Figure 8* for bulk polymerization (full curves) and for solution polymerization at c = 20% (dotted curves), using an AIBN concentration of 0.08 M. For bulk polymerization and with less than 0.3% DVB, the reaction system becomes glassy prior to the onset of gelation. For solution polymerization (20%), no gelation occurs below 1% DVB owing to the insufficient amount of DVB. The conversion of the vinyl groups at t_g decreases abruptly as the concentration of DVB increases and then levels off. A decrease in the total monomer concentration c or an increase in the AIBN concentration (not shown in *Figure 8*) will shift the gel point to higher conversions, i.e. gelation occurs later.

The effect of the AIBN concentration on the variation

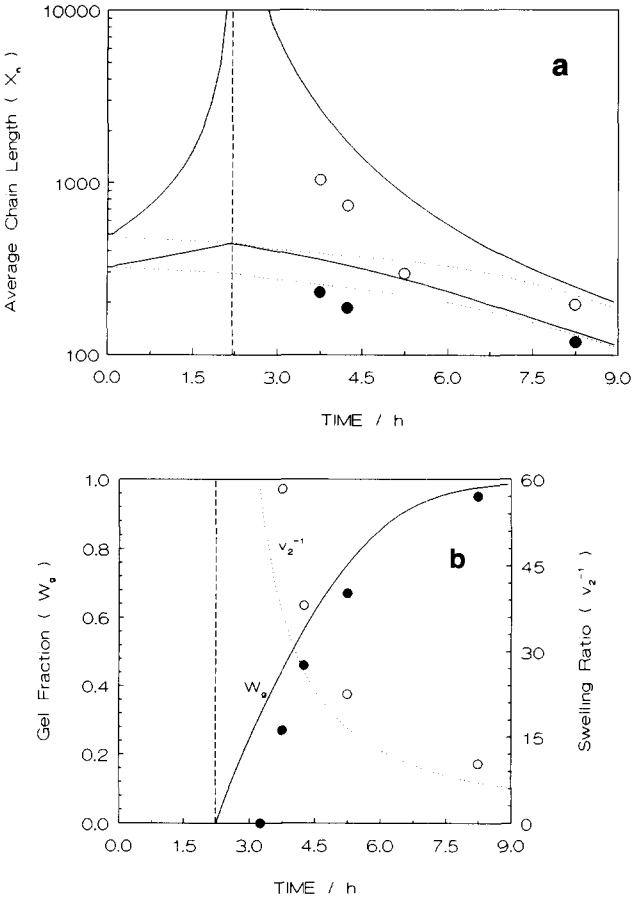

Figure 7 (a) Variation of the average polymerization degrees of the primary molecules (dotted curves) and the branched molecules (full curves) with the reaction time. Experimental results of Hild *et al.* for $\bar{X}_1$ and $\bar{X}_2$ are shown as filled and empty circles respectively. (b) Variation of the gel fraction W_g and the equilibrium swelling ratio of the gel in toluene v_2^{-1} with the reaction time. Experimental results of Hild *et al.* for W_g and v_2^{-1} are shown as filled and empty circles respectively. Calculations are for m = 2, DVB = 5%, c = 43%, $[I]_0$ = 0.08 M

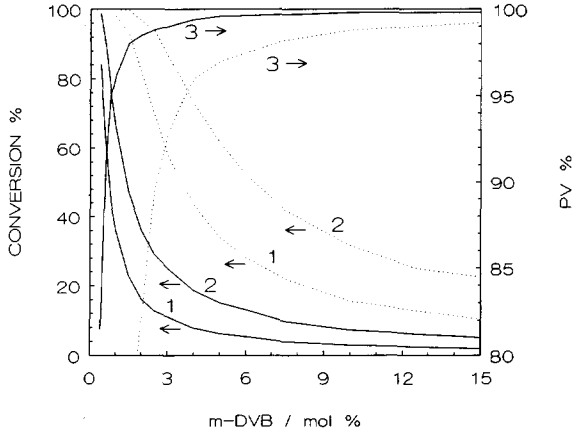

Figure 8 Effect of the *m*-DVB concentration on the critical conversion of the vinyl groups M_1 (1) and M_2 (2) and on the fraction of DVB units bearing pendent vinyls at t_g (3) for bulk polymerization (full curves) and solution polymerization at $c=20\%$ (dotted curves). $[I]_0=0.08$ M

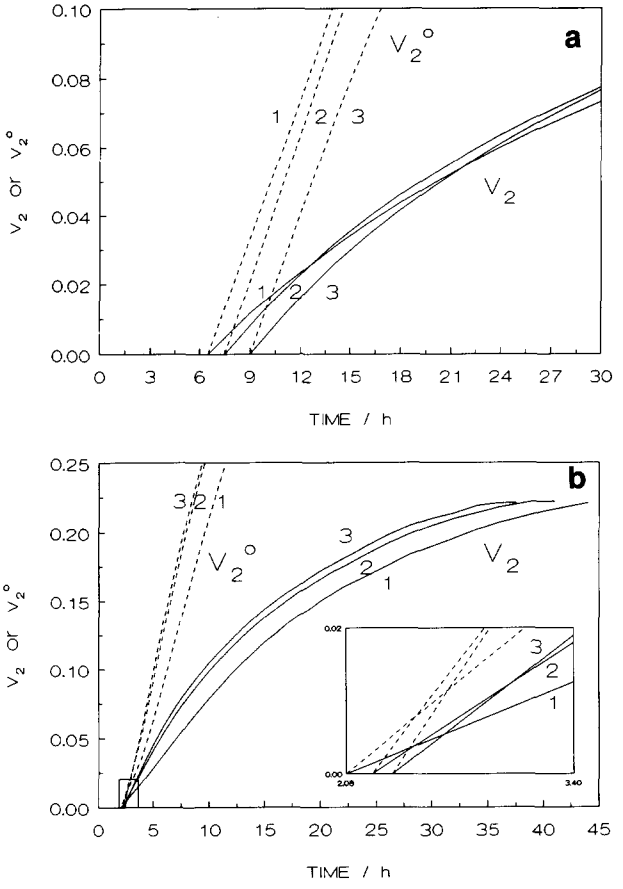

Figure 9 Effect of the AIBN concentration on the variation of v_2 (full curves) and v_2° (broken curves) with the reaction time for (a) 2% and (b) 5% DVB. $c=50\%$, $[I]_0=0.02$ M (1), 0.08 M (2) and 0.14 M (3). Calculations are for $m=1$. The inset in (b) is a magnification of the small box

of the volume swelling ratio of S–DVB networks *versus* reaction time is shown in *Figure 9* for $c=50\%$. The initial concentration of DVB is 2% in *Figure 9a* and 5% in *Figure 9b*. The broken curves represent the degree of dilution of the networks (v_2°). Simulations were carried out for $m=1$ and continued until total conversion of the vinyl groups M_1 and M_2. As the initial concentration of AIBN increases, gelation is delayed; therefore, as seen from *Figure 9a* and from the inset of *Figure 9b*, the loosely crosslinked networks formed just beyond gelation or those obtained at high AIBN and low DVB contents exhibit a decrease in v_2, i.e. an increase in the swelling ratio with increasing AIBN concentration. However, given a reaction time sufficient for network formation, v_2 becomes directly proportional to the AIBN concentration owing to the increase in the rate of change of v_2 with time as the radical concentration increases. The limiting v_2 values, i.e. those obtained at the total conversion of M_1 and M_2 vinyls, are not greatly affected by the initiator concentration.

From the practical point of view, it is interesting to extend the above calculations to include highly crosslinked S–DVB networks, although the calculated results will be only qualitatively acceptable. In *Figure 10*, the variation of v_2 and v_2° with the reaction time is shown for $c=50$ and 20%. The initial concentrations of DVB and AIBN are 80 mol% (with respect to the monomers) and 0.08 M respectively. It can be seen that v_2 reaches the value of v_2°, in other words, the incipient phase separation occurs, after 0.33 h, i.e. at t_g, and after 2.13 h for $c=20$ and 50% respectively. Moreover, phase separation occurs earlier as the initial concentration of AIBN increases (*Figure 11*); for $c=50\%$, the reaction time for incipient phase separation decreases from 2.13 to

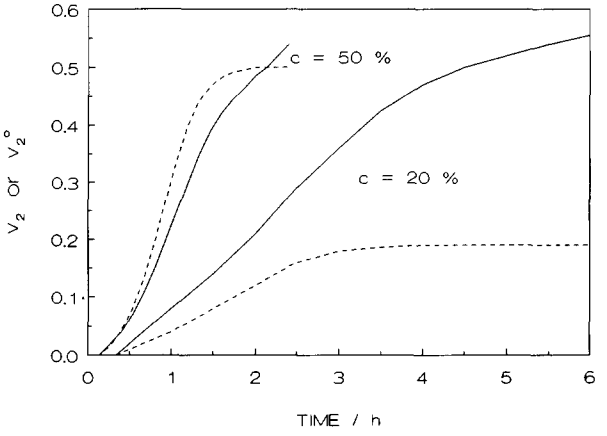

Figure 10 Variation of v_2 (full curves) and v_2° (broken curves) with the reaction time for $c=50$ and 20%. DVB=80%, $[I]_0=0.08$ M. Simulations were for $m=1$ and carried out until the total conversion of monomeric vinyls

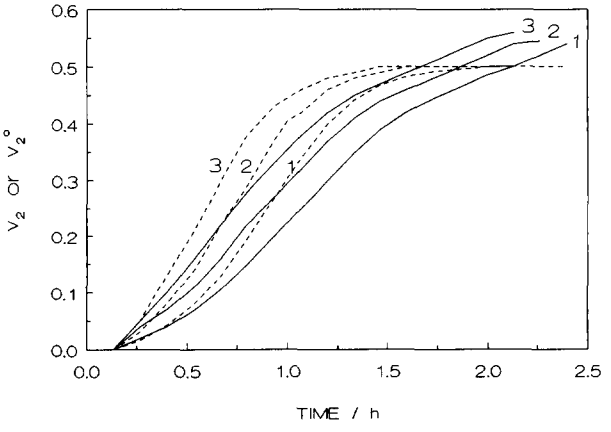

Figure 11 Effect of the AIBN concentration on the variation of v_2 (full curves) and v_2° (broken curves) with the reaction time for 80% DVB and $c=50\%$. $[I]_0=0.08$ M (1), 0.32 M (2) and 1 M (3). $m=1$

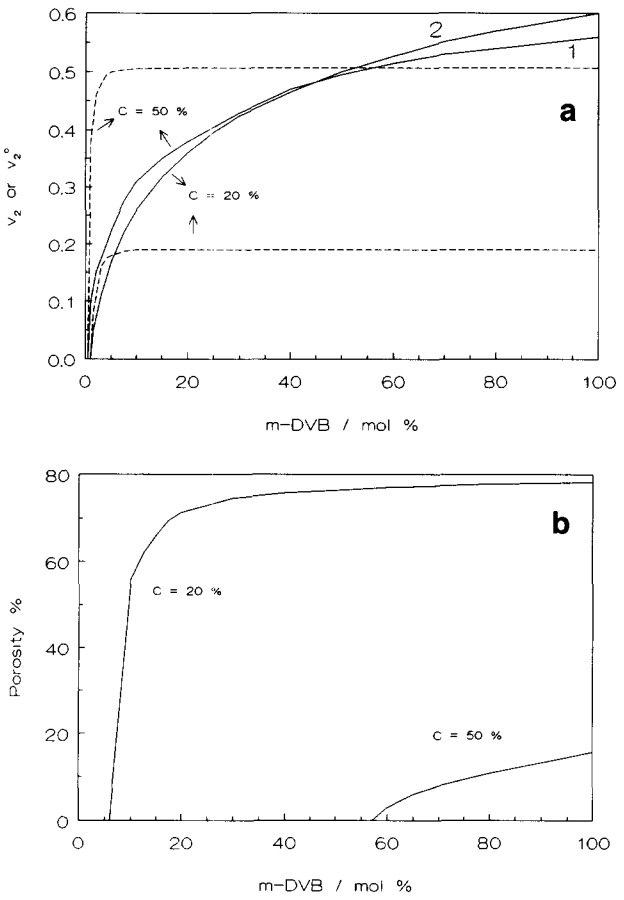

Figure 12 Effect of the initial DVB concentration on (a) the limiting v_2 (full curves) and v_2° values (broken curves) and (b) the porosity of the networks. $c = 50\%$ (1) and 20% (2), $m = 1$

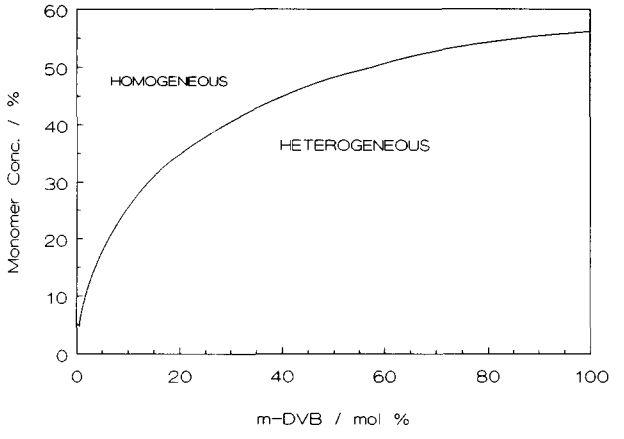

Figure 13 Relationship between the threshold concentration of *m*-DVB and the monomer concentration

1.67 h as the AIBN concentration increases from 0.08 to 1 M.

Figure 12a illustrates the dependence of the limiting v_2 and v_2° values on the DVB concentration for $c = 50$ and 20%. In *Figure 12b*, the porosities of these networks are plotted as a function of the DVB concentration. It is seen that for the onset of phase separation, i.e. for the formation of heterogeneous structures, a threshold concentration of the DVB is necessary. The threshold concentrations of DVB for phase separation are 6 and 57% for $c = 20$ and 50% respectively. Below the threshold concentration, the reaction system is in a single homogeneous phase for all AIBN concentrations. As DVB is increased beyond this value, phase separation occurs. Depending on the threshold concentrations, the regions for the formation of homogeneous and heterogeneous structures are calculated and given in *Figure 13*.

Within the past 30 years, significant experimental effort has been made to synthesize heterogeneous networks[9,40]. Experimental results clearly show that heterogeneous S–DVB networks are obtained only above certain threshold concentrations of the diluent and of the DVB. The higher the DVB concentration, the lower is the threshold concentration of the diluent. The porosity of S–DVB networks increases as the concentration of the DVB or of the diluent increases. *Figures 10–13* show exactly these trends.

CONCLUSIONS

A kinetic model was developed for free-radical MVM–DVM copolymerization reactions. Useful average properties were derived as a function of reaction time. The moment equations based on the primary molecules appear to be more powerful than those based on the branched molecules; they can also be used to calculate the structural characteristics of the gel, such as the cycle-rank density. Two major transitions of network-forming systems, namely gelation and phase separation, were predicted. Simplified equations for calculating the number- and weight-average polymerization degrees of branched polymers and the gel-point condition are identical to the equations derived by Flory and Stockmayer using statistical methods. Comparison of the model predictions with the experimental data of Hild and Okasha encourages the expectation that the model may be applicable to the enormous systems of practical interest.

It must be noted that several restrictions were introduced during the development of the present model. A more realistic kinetic model of MVM–DVM copolymerization would require the treatment of cyclization[43], crosslink-density distribution[17], changes in k_{p3} depending on the size of the molecule bearing the pendent vinyl, as well as the calculation of the initial condition of the moment equations at the point of gelation. However, the idealized kinetic model presented in this paper is thought to form the basis for treating these deviations. Because of the simplicity of the relations derived, it is expected that these relations can be further developed theoretically, or empirically from the magnitude of deviations observed in real systems.

REFERENCES

1 Flory, P. J. *J. Am. Chem. Soc.* 1941, **63**, 3083, 3091, 3096
2 Flory, P. J. 'Principles of Polymer Chemistry', Cornell University Press, Ithaca, NY, 1953, Ch. 9
3 Stockmayer, W. H. *J. Chem. Phys.* 1943, **11**, 45
4 Stockmayer, W. H. *J. Chem. Phys.* 1944, **12**, 125
5 Gordon, M. *Proc. R. Soc. Lond.* (*A*) 1962, **268**, 240
6 Macosko, C. W. and Miller, D. R. *Macromolecules* 1976, **9**, 199
7 Miller, D. R. and Macosko, C. W. *Macromolecules* 1976, **9**, 206
8 Durand, D. and Bruneau, C.-M. *Makromol. Chem.* 1982, **183**, 1007, 1021
9 Dusek, K. in 'Developments in Polymerization – 3' (Ed. R. N. Haward), Applied Science, London, 1982, p. 143
10 Dusek, K. *Br. Polym. J.* 1985, **17**, 185
11 Dusek, K. *J. Macromol. Sci.–Chem.* (*A*) 1991, **28**, 843
12 Sarmoria, C. and Miller, D. R. *Macromolecules* 1991, **24**, 1833

13 Dotson, N. A. *Macromolecules* 1992, **25**, 308
14 Charmot, D. and Guillot, J. *Polymer* 1992, **33**, 352
15 Mikos, A. G., Takoudis, C. G. and Peppas, N. A. *Macromolecules* 1986, **19**, 2174
16 Tobita, H. and Hamielec, A. E. *Makromol. Chem., Macromol. Symp.* 1988, **20/21**, 501
17 Tobita, H. and Hamielec, A. E. *Macromolecules* 1989, **22**, 3098
18 Tobita, H. and Hamielec, A. E. *Makromol. Chem., Macromol. Symp.* 1990, **35/36**, 193
19 Zhu, S., Tian, Y., Hamielec, A. E. and Eaton, D. R. *Polymer* 1990, **31**, 154
20 Tian, Y., Zhu, S., Hamielec, A. E., Fulton, D. B. and Eaton, D. R. *Polymer* 1992, **33**, 384
21 Odian, G. 'Principles of Polymerization', McGraw-Hill, New York, 1981, Ch. 6
22 Malinsky, J., Klaban, J. and Dusek, K. *J. Macromol. Sci.–Chem. (A)* 1971, **5**, 1071
23 Hild, G. and Rempp, P. *Pure Appl. Chem.* 1981, **53**, 1541
24 Hild, G., Okasha, R. and Rempp, P. *Makromol. Chem.* 1985, **186**, 407
25 Tobita, H. and Hamielec, A. E. *Polymer* 1992, **33**, 3647
26 Tobita, H. *Macromolecules* 1992, **25**, 2671
27 Flory, P. J. *Br. Polym. J.* 1985, **17**, 96
28 Flory, P. J. *Macromolecules* 1979, **12**, 119
29 Erman, B. and Flory, P. J. *Macromolecules* 1986, **19**, 2342
30 Flory, P. J. *Discuss. Faraday Soc.* 1970, **49**, 7
31 Dusek, K. and Prins, W. *Adv. Polym. Sci.* 1969, **6**, 1
32 Galina, H., Kolarz, B. N., Wieczorek, P. P. and Wojczynska, M. *Br. Polym. J.* 1985, **17**, 215
33 Okay, O. *J. Appl. Polym. Sci.* 1986, **32**, 5533
34 Fox, T. G. and Loschaek, S. *J. Polym. Sci.* 1955, **15**, 391
35 Ellis, T. S., Karasz, F. E. and Ten Brinke, G. *J. Appl. Polym. Sci.* 1983, **28**, 23
36 Hild, G. and Okasha, R. *Makromol. Chem.* 1985, **186**, 93
37 Orwoll, R. A. *Rubber Chem. Technol.* 1977, **50**, 451
38 Erman, B. and Baysal, B. M. *Macromolecules* 1985, **18**, 1696
39 Carpenter, M. R., Davies, D. B. and Matheson, A. J. *J. Chem. Phys.* 1967, **46**, 2451
40 Seidl, J., Malinsky, J., Dusek, K. and Heitz, W. *Adv. Polym. Sci.* 1967, **5**, 113
41 Hasa, J. and Janacek, J. *J. Polym. Sci. (C)* 1967, **16**, 317
42 Bates, R. F. and Howard, G. J. *J. Polym. Sci. (C)* 1967, **16**, 921
43 Landin, D. T. and Macosko, C. W. *Macromolecules* 1988, **21**, 846

APPENDIX 1

Calculation of the mole fraction of the radical species x_j

Invoking the steady-state approximation for each of the radical species separately, and assuming that the propagation rates are much larger than both the initiation and termination rates, one obtains:

$$x_1 : x_2 : x_3 = 1 : a : b$$

where

$$a = \frac{k_{p12}[M_2]\{k_{p31}[M_1] + k_{p32}[M_2] + (k_{p13}k_{p32}/k_{p12})[M_3]\}}{k_{p21}[M_1]\{k_{p31}[M_1] + k_{p32}[M_2] + (k_{p31}k_{p23}/k_{p21})[M_3]\}}$$

$$b = \frac{(k_{p13} + ak_{p23})[M_3]}{k_{p31}[M_1] + k_{p32}[M_2]}$$

APPENDIX 2

Derivation of the moment equations

Invoking the steady-state approximation, the moments of the *primary* molecules in the sol can be derived as follows.

Radical balances

$$r_{R_1'^*} = \sum_{i=1}^{3} k_{ai}[A^*][M_i'] - \left(\sum_{i=1}^{3} k_{pi}[M_i] + k_t[R^{\bullet *}] \right)[R_1'^*] \simeq 0 \qquad \text{(A1a)}$$

$$r_{R_r'^*} = \sum_{i=1}^{3} k_{pi}[M_i']([R_{r-1}'^*] - [R_r'^*]) - (k_{p3}[M_3''] + k_t[R^{\bullet *}])[R_r'^*] \simeq 0 \qquad r = 2, 3, 4, \ldots \qquad \text{(A1b)}$$

Radical moments

$$r_{Y_n^\bullet} = k_t[R^{\bullet *}]^2 + \sum_{i=1}^{3} k_{pi}[M_i'] \sum_{v=0}^{n-1} \binom{n}{v} Y_v^\bullet - (k_{p3}[M_3''] + k_t[R^{\bullet *}])Y_n^\bullet \simeq 0 \qquad n = 0, 1, 2, \ldots \qquad \text{(A2)}$$

Polymer balances Eliminating the balance of radicals, the balance equation for sol polymers can be written as follows:

$$r_{P_r'^\bullet} = k_{td}[R^{\bullet *}][R_r'^*] + 0.5k_{tc} \sum_{s=1}^{r-1} [R_s'^*][R_{r-s}'^*] \qquad r = 1, 2, 3, \ldots \qquad \text{(A3)}$$

Polymer moments

$$r_{Q_n^\bullet} = k_{td}[R^{\bullet *}]Y_n^\bullet + 0.5k_{tc} \sum_{v=0}^{n} \binom{n}{v} Y_v^\bullet Y_{n-v}^\bullet \qquad n = 0, 1, 2, \ldots \qquad \text{(A4)}$$

Since $Y_n^\bullet \gg Y_{n-1}^\bullet$ and

$$\sum_{i=1}^{3} k_{pi}[M_i'] \simeq \sum_{i=1}^{3} k_{pi}[M_i]$$

in free-radical polymerization, the moment equations given above yield equations (12) and (13) in the text.

The moments of the *branched* molecules are evaluated as follows:

Radical balances

$$r_{R_i'^*} = \sum_{i=1}^{2} k_{ai}[A^*][M_i] - \left(\sum_{i=1}^{3} k_{pi}[M_i] + k_t[R^*] \right)[R_1'^*] \simeq 0 \qquad \text{(A5a)}$$

$$r_{R_r'^*} = k_{a3}[A^*][M_{3,r-1}'] + \sum_{i=1}^{2} k_{pi}[M_i]([R_{r-1}'^*] - [R_r'^*]) + \sum_{j=1}^{r-2} k_{p3}[M_{3,j}'][R_{r-j-1}'^*] - (k_{p3}[M_3] + k_t[R^*])[R_r'^*] \simeq 0 \qquad r = 2, 3, 4, \ldots \qquad \text{(A5b)}$$

Radical moments

$$r_{Y_n} = k_t[R^*]^2 + \sum_{i=1}^{2} k_{pi}[M_i] \sum_{v=0}^{n-1} \binom{n}{v} Y_v + \sum_{v=0}^{n-1} k_{p3}[M_3'] \binom{n}{v} Y_v Q_{n+1-v}/Q_1 - (k_{p3}[M_3''] + k_t[R^*])Y_n \simeq 0 \qquad n = 0, 1, 2, \ldots \qquad \text{(A6)}$$

Polymer balances

$$r_{P'_r} = k_{td}[R^*][R'^*_r] + 0.5k_{tc}\sum_{s=1}^{r-1}[R'^*_s][R'^*_{r-s}] - k_{p3}[M'_{3,r}][R'^*] \qquad r = 1, 2, 3, \ldots \qquad (A7)$$

Polymer moments

$$r_{Q_n} = k_{td}[R^*]Y_n + 0.5k_{tc}\sum_{\nu=0}^{n}\binom{n}{\nu}Y_\nu Y_{n-\nu} - k_{p3}[M'_3]Y_0 Q_{n+1}/Q_1 \qquad n = 0, 1, 2, \ldots \qquad (A8)$$

The approximations made for the primary molecules yield the equations in the text.